Journal of Hydrology: Regional Studies 32 (2020) 100752

Contents lists available at ScienceDirect

Journal of Hydrology: Regional Studies

journal homepage: www.elsevier.com/locate/ejrh

On the relationship between reversal of the river stage (repiquetes), rainfall and low-level wind regimes over the western Amazon basin

Manuel Figueroa [a,*], Elisa Armijos [a], Jhan Carlo Espinoza [b], Josyane Ronchail [c], Pascal Fraizy [d]

[a] Instituto Geofísico del Perú, Calle Badajoz #169, Mayorazgo IV Etapa, Ate Vitarte, Lima, Peru
[b] Univ. Grenoble Alpes, IRD, CNRS, G-INP, IGE (UMR 5001), 38000 Grenoble, France
[c] Paris University and Laboratory of Climate and Oceanography - LOCEAN (Sorbonne University, IRD, MNHN, CNRS), 4 Place Jussieu, 75252 Paris Cedex 05, France
[d] IRD, Géoscience Environnement Toulouse (GET-CNRS, IRD, Université de Toulouse), Toulouse, France

ARTICLE INFO

Keywords:
Repiquetes
Rainfall
Circulation patterns
Recessional agriculture
Western Amazon

ABSTRACT

Study region: The Amazonas River and its tributaries (Peru), where riparian farmers face hydrological events that put their lowland crops at high risk of production loss during the flood recession period.
Study focus: This paper analyzes the hydro-meteorological mechanisms over the Andes-Amazon basins that produce "repiquetes", which are sudden reversals of the river stage. They are defined and characterized for the period 1996–2018 by using river stage data from three hydrological gauging stations for the Amazonas, Marañón and Ucayali Rivers. Daily rainfall and low-level winds depict the large-scale atmospheric patterns associated with repiquetes.
New hydrological insights: Among 73 significant repiquetes (reversal $\geq$ 20 cm) observed in the Amazonas River, 64 % were preceded by repiquetes only in the Marañón River, 5 % by repiquetes only in the Ucayali River, 21 % by repiquetes in both rivers and 10 % was only registered in the Amazonas River without upstream precursor. These results show that repiquetes in the Marañón River are the primary precursors of repiquetes in the Amazonas River. Most repiquetes are associated with abundant rainfall over the Peruvian and Ecuadorian Andes-Amazon transition region related to a remarkable change in the direction of the meridional wind, from north to south, and an easterly flow five to three days before the beginning of a repiquete in the Amazonas River.

1. Introduction

Most of the Andean rivers within the Amazon basin of Peru and Ecuador flow into the Amazonas River, which is formed by the confluence of the Ucayali and Marañón Rivers. At Tamshiyacu station, the first hydrological station in Amazonas River (Fig. 1a), a mean discharge of about 32,000 m^3/s is estimated (Espinoza et al., 2009a). The Andean-Amazon hydrological basin upstream of

* Corresponding author.
E-mail addresses: mfigueroa9418@gmail.com (M. Figueroa), earmijos@igp.gob.pe (E. Armijos), jhan-carlo.espinoza@univ-grenoblealpes.fr (J.C. Espinoza), josyane.ronchail@locean-ipsl.fr (J. Ronchail), pascal.fraizy@ird.fr (P. Fraizy).

https://doi.org/10.1016/j.ejrh.2020.100752
Received 3 April 2020; Received in revised form 9 October 2020; Accepted 13 October 2020
Available online 2 November 2020

Tamshiyacu station (hereafter, Tamshiyacu basin) covers 726,400 km^2.

Downstream the confluence of the Ucayali and Marañón Rivers and near to the city of Iquitos, riparian communities practice riverine agriculture. They take advantage of the falling water level of the flooding cycle to cultivate in the exposed riverbed, floodplains and point bars during annual recession (Hiraoka, 1985; Rios Arevalo, 2005; Coomes et al., 2016; List, 2016; List and Coomes, 2017; Ronchail et al., 2018) since the soils are enriched by sediment transport from the Andes (McClain and Naiman, 2008). Riparian farmers grow crops with a shorter growing season like rice and cowpea on the active channel, taking into account the elevation of the river and the date in order to choose reliable seed varieties, and they grow plantain, maize, and manioc on the levees (List and Coomes, 2017). However, there are crucial factors that affect crop production, such as poor soil, early flooding and unpredictable stage reversals (or interruptions of the recession limb of the annual hydrograph) known as "repiquetes" (List, 2016; List and Coomes, 2017). Coomes et al. (2016) defined repiquetes as unexpected reversal or inversions in direction (sign) of water level equal or greater than 1 cm, and studied their effect on crop loss on the floodplain communities near the city of Iquitos. The repiquetes affect farmers' livelihoods and are associated with high crop loss due to either crop damage or seeds being washed away, and often, farmers have nothing more to plant (i.e. they caused a reduction of the household potential outputs) (List and Coomes, 2017). Later, Ronchail et al. (2018) found evidence of a lengthening of the low water period since the eighties and linked repiquetes events to unusually high rainfall over the Tamshiyacu basin during the week leading up to these events in Tamshiyacu.

Regarding the high impacts of repiquetes on riverine communities in the Peruvian Amazon, the first objective of this study is to characterize the occurrence of repiquetes over the main tributaries of the Amazonas River at Tamshiyacu in terms of frequency, duration, magnitude and timing. In addition, repiquetes in the Ucayali and Marañón Rivers are analyzed to define precursors of those in the Amazonas River.

Due to its meridional extension from the southern tropics to the equator and its complex topography, the Peruvian and Ecuadorian Amazon basin is characterized by a striking rainfall contrast. The highest values occur towards the equator and on the eastern slopes of the Andes, especially under windward conditions between 1000–1500 masl, while low rainfall values occur in the southern part of the basin and over the mountains, generally above 2500 masl (Killeen et al., 2007; Espinoza et al., 2009b, 2015; Chavez and Takahashi, 2017). In addition, rainfall variability over this region is modulated by dynamic and thermodynamic atmospheric variability that occurs on a regional and local scale, covering a multitude of timescales (see Section 2). These characteristics make short-term flow forecasts challenging in the Peruvian-Ecuadorian Amazon basin. In this context, our second objective is to identify rainfall and large-scale atmospheric circulation patterns related to the occurrence of repiquetes events. These objectives are oriented towards providing information for the mitigation risk of crop loss in the region as well as scientific bases to improve the accuracy of flow forecasts in the Peruvian-Ecuadorian Amazon basin.

2. Data and methods

2.1. Study Area and main climatic features

Over the western Amazon, two of the major andean-amazonian rivers, the Ucayali and the Marañón Rivers flow into the Amazonas River 80 km from the city of Iquitos, Peru (Fig. 1a). The Amazonas River is considered an anabranching river with high migration rates of meanders near its origin (Kalliola et al., 1992). Moreover, Abad et al. (2013) classified the Ucayali and Marañón Rivers as a

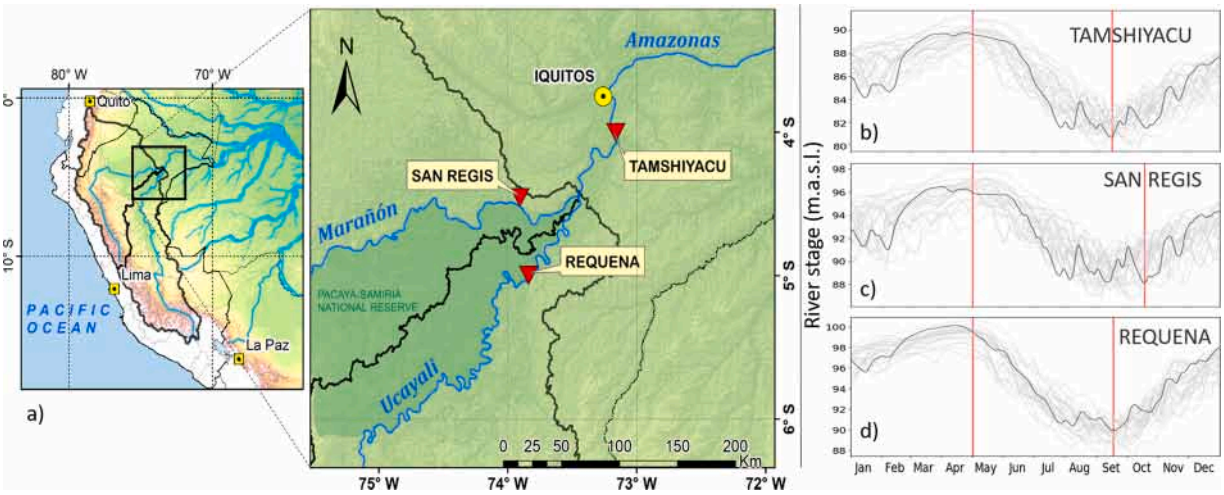

Fig. 1. a) Location of the gauging stations in the Peruvian Amazon: San Regis on the Marañon River, Requena on the Ucayali River and Tamshiyacu on the Amazonas River. Items b), c) and d) show hydrograms of the Amazonas, Marañon and Ucayali Rivers, respectively. Gray lines display daily average river stages in each station for the 1996–2018 period. The black line corresponds to the daily river stage in 1997. Red vertical lines define the minimum and maximum daily river stage of 1997.

meandering river and an anabranching river, respectively. The Ucayali and the Marañón Rivers have a mean discharge of 13,500 m^3/s and 14,900 m^3/s and their basins have an areal extent of about 350,000 km^2 and 362,000 km^2, respectively (Espinoza et al., 2009a; Lavado Casimiro et al., 2013).

Precipitation over this region is characterized by complex annual cycle regimes (Espinoza et al., 2020 and references therein). Previous studies have shown a seasonal rainfall distribution over the northwest equatorial Amazon region, especially over Peru, Ecuador, and Colombia, with a somewhat marked bimodal regime. A peak with slightly more rainfall is observed during February-May in relation to enhanced convection due to the southward displacement of the Intertropical Convergence Zone (ITCZ) and another relative peak in October-November is associated with westward moisture transport (Laraque et al., 2007; Espinoza et al., 2009b; Segura et al., 2019). Conversely, over the central and southern Peruvian Amazon basin, the seasonal cycle of precipitation has a marked dry season (May to September) and a peak in December to March related to the mature phase of the South American Monsoon System (SAMS; Vera et al., 2006). In addition, the South American low-level jet east of the Andes (LLJ) enhances moisture transport from the tropical Atlantic Ocean and the tropical rainforest to the southern Amazon and subtropical South America (Marengo et al., 2004). Likewise, Laraque et al. (2007) have documented the complex relationship between rainfall regimes and streamflow regimes over the equatorial Andes, especially over the Santiago, Pastaza, and Napo basins (Ecuadorian and Peruvian upper Amazon sub-basin).

The above-described rainfall seasonality over the basin explains the annual cycle of discharge in the Ucayali, Marañón and Amazonas Rivers, at Requena, San Regis and Tamshiyacu stations, respectively (Fig. 1). There are two seasons defined by their river stage: i) the high stage with high water levels of the river, generally during March-April, related to the abundant rainfall during the austral summer (December to March) over the central and southern part of the Peruvian Amazon (Espinoza et al., 2009a; Lavado Casimiro et al., 2013), and ii) the low stage with low water levels between September-October, associated with low rainfall rates during the austral winter especially in the southern region (Espinoza et al., 2011; Coomes et al., 2016; Ronchail et al., 2018). In addition, it is important to note that the discharge of the Marañón River is twice the discharge of the Ucayali River from June to October (Armijos et al., 2013). The mean difference between low and high water levels is approximately seven meters at Tamshiyacu station (Ronchail et al., 2018). This seasonal variation in water level is already taken into account by the riparian communities which practice riverine agriculture during the falling water season. However, unpredictable stage reversals during falling water levels are among the main risks that affect riparian farmers and their crops along the Peruvian Amazon River.

The day to day rainfall variability over the Peruvian Ecuadorian Amazon basin is modulated by a complex interaction between atmospheric circulation and the Andean orography, involving several dynamic and thermodynamic processes acting from the local to the large scale (Satyamurty et al., 1998; Wang and Fu, 2002; Kiladis et al., 2009; Espinoza et al., 2012; Paccini et al., 2017; Mayta et al., 2018; Recalde-Coronel et al., 2020). Wang and Fu (2002) described that the cross-equatorial flow at low-levels is more frequently from the south (north) when it rains over the equatorial regions (southern Amazon). According to the above-mentioned studies, the mechanisms responsible for the cross-equatorial regimes vary on different timescales. On a sub monthly timescale, the variability of the cross-equatorial regime could be related to easterly waves, equatorial waves, Madden-Julian Oscillation, among others.

On the other hand, Paccini et al. (2017) defined nine large-scale atmospheric circulation patterns (CPs) from meridional and zonal winds to identify the main intra-seasonal meteorological features over the Amazon basin by using hierarchical ascendant classification and Self-Organizing Maps. Subsequently, these nine CP's are classified in terms of types of dominant low level circulations over the Amazon basin into northerly wind regimes (CP2, CP8 and CP9), southerly wind regimes (CP4, CP5 and CP6) and intermediate states (CP1, CP3, CP7), but each one with different zonal wind characteristics. Finally, the CP4 is the rainiest CP over the Peruvian and Ecuadorian Amazon at Tamshiyacu station, and opposite conditions are observed during the CP5. Such a difference between southerly regimes can be explained by a much greater westerly flow in CP5 related to rainfall over the eastern Amazon basin. However, the relationship between large-scale intraseasonal atmospheric circulation patterns and changes in the Amazonas River stage has not been documented previously and this work is an attempt to look for proxies to improve streamflow forecasting.

2.2. Hydro-climatic data

2.2.1. River stages and stream velocity

Daily river stages are analyzed in three hydrological stations: Requena on the Ucayali River, San Regis on the Marañón River and Tamshiyacu on the Amazonas River, located upstream from the city of Iquitos (Fig. 1a). Similarly, the downstream distance between

Table 1
Mean stream velocity (m/s) and standard deviation (std) of the river section measured with Acoustic Doppler Current Profiler (ADCP), where *n* is the total of field measurements, and *t* is the number of transects. Measures were conducted during low stage season (from May to October) during the 2002–2011 period.

Station		may	jun	jul	aug	set	oct
San Regis	mean	1.56	1.5	1.45	1.13	1.04	1.1
	std	0.02	0.02	0.04	0.02	0.02	0.02
	n	9	3	1	3	3	5
	t	49	12	5	19	14	23
Requena	mean	1.35	1.09	0.92	0.5	0.54	0.73
	std	0.05	0.01	0.03	0.01	0.02	0.02
	n	6	4	1	2	2	5
	t	39	21	4	11	10	19

San Regis and Tamshiyacu station is approximately 150 km and between Requena and Tamshiyacu station 220 km. River stages are provided by the Environmental Observatory SO-Hybam and the National Service of Meteorology and Hydrology of Peru (SENAMHI). This information is available at http://www.ore-hybam.org. Tamshiyacu and San Regis river stages data cover the period 1985−2018. However, Requena station has a shorter time series from July 1996 to December 2018.

Stream velocity was computed in each hydrological station using the cross-section velocity measured with the Acoustic Doppler Current Profiler (ADCP) in the low water season of the 2002–2011 period (http://www.ore-hybam.org). Stream velocity is the mean of the number (N) of field measurements in which the ADCP measured at least four transects along a stretch of the river (Table 1).

2.2.2. Rainfall data

In this study, two rainfall datasets have been used:

i) Climate Hazards Group InfraRed Precipitation with Station v.2 (CHIRPS v.2; Funk et al., 2015) daily data with 0.05° and 0.25° spatial resolutions, covering the 1996–2018 period. This dataset is a combination of global rain gauge data (containing a large number of observations from Brazil, Colombia, Peru and others countries) and satellite precipitation estimates using a regression method from global daily cold cloud duration values and calibration using the Tropical Rainfall Measurement Mission (TRMM) product 3B42 V.7 (TRMM-3B42 V.7). Moreover, CHIRPS v.2 has been evaluated over this region by previous studies (Paccini et al., 2017; Wongchuig Correa et al., 2017; Espinoza et al., 2018; Recalde-Coronel et al., 2020). This dataset was used for the period 1996–2018.
ii) TRMM-3B42 V.7 quasi-global dataset, which has a 0.25° spatial resolution, has been widely used for hydro-meteorological research in the Peruvian Amazon basin (Zulkafli et al., 2014; Zubieta et al., 2015; Paccini et al., 2017; Wongchuig Correa et al., 2017). This dataset was used considering the period 1998-2018.

2.2.3. Atmospheric circulation data

Atmospheric circulation was analyzed using both meridional and zonal winds at 850 hPa from the European Centre for Medium-Range Weather Forecasts reanalysis ERA-Interim (Dee et al., 2011), over the region defined by 45 °S–15 °N, 85−30 °W. This data set was used for the 1996–2018 period, with a spatial resolution of 0.25° × 0.25°. The horizontal wind components at 850 hPa have been used in studies related to the atmospheric patterns over the Andes-Amazon basin (Espinoza et al., 2012; Paccini et al., 2017; Santos et al., 2015; Segura et al., 2019; Ampuero et al., 2020). Moreover, the structure of the atmosphere in the eastern Andes is described using ERA-Interim (0.25°) temperature, specific humidity, relative humidity, vertical velocity and horizontal winds at 1000, 950, 925, 850, 700, 600, 500, 300 and 200 hPa.

2.3. Definition and classification of repiquetes

The study focuses on the annual recession and the low water period (generally from May to October; Espinoza et al., 2011; Ronchail et al., 2018). The repiquetes were calculated individually for each gauging station within each year as follows:

i) The maximum value of daily river stage after May 1st and the minimum value during the low water stage, before November 1st, are identified to define the annual recession (Fig. 1b). The choice of these dates is based on a) the mean annual cycle of the river stage at Tamshiyacu station and b) the impact of the repiquetes on downstream recessional agriculture, considering that this period includes the mean planting dates that range from June 11th to June 25th and the growing season (75–150 days) of most rice varieties (Coomes et al., 2016; List and Coomes, 2017). Examples of annual recession defined for the year 1997 are between the red lines (beginning and final days) in Figs. 1b–d and S1 (Supplementary Material).
ii) The river stage on the first day of the repiquete must be higher than on the preceding day (day zero – d0), i.e., when there is a positive reversal of the stage. In addition, the last day of the repiquete is when the river stage returns to the same value (or lower) than the stage of d0, except the last annual repiquete. Considering the last repiquete of the year, d0 corresponds to the lowest annual river stage and concludes when the river stage stops rising (Fig. S1). Note that this study focuses on repiquetes during the annual recession; the rising period has not been analyzed.

After the identification of repiquetes in each river, they are characterized according to their magnitude, duration and timing (Ronchail et al., 2018). The magnitude (in cm) corresponds to the maximum value of the reversal throughout the entire duration of the event. The duration of the repiquete is the period (in days) between d0 and the last day defined above. Fig. S1 shows a sketch that defines and illustrates the characteristics of repiquetes. Subsequently, values greater than or equal to 10 cm for the Ucayali and Marañón Rivers, and 20 cm for the Amazonas River were taken as thresholds for events with potential impacts on farming activities in the Amazon plain, as well as to look for a relationship with rainfall and circulation anomalies during the preceding days. The 20 cm threshold used in the Amazonas River has been documented by previous studies based on its impact on crops (Coomes et al., 2016; Ronchail et al., 2018). A lower value (10 cm) has been chosen for the San Regis and Requena stations in order to reduce failure in detecting events that may cause relevant changes in the water level at Tamshiyacu station.

First, the repiquetes of each station were arranged chronologically. Then, to match events that occur upstream with those that occur downstream, a delay (in days) was considered using the minimum stream velocity and the calculated distances between Requena or San Regis and Tamshiyacu (Table 1). We consider these delays to represent the maximum time of wave propagation for each river. Hence, the repiquetes that are supposed to trigger the beginning of an event at Tamshiyacu occur the same day up to three days before

in the Marañón River and up to six days before in the Ucayali River. Also, we used a cross-correlation method (Lee et al., 2006; Guevara Díaz, 2014) to compare results with the delay obtained above. In the same way, using the cross-correlation method, we obtained one day for the Marañón and four days for the Ucayali. However, as this method involves raw time series that includes the high level water period, we decided to use a longer period of time between the two methods: from zero to three (six) days prior in the Marañón (Ucayali) River.

This approach allows us to identify "types" of repiquetes in Tamshiyacu as a function of their precursors on the Marañón or Ucayali Rivers. Thus, we identify four types of repiquetes: Type 1 (repiquetes observed in Tamshiyacu with a precursor in the Marañón River at San Regis), Type 2 (repiquetes observed in Tamshiyacu with a precursor in the Ucayali River at Requena), Type 3 (repiquetes observed in Tamshiyacu with precursors in both tributaries) and Type 4 (repiquetes observed in Tamshiyacu and not detected upstream).

2.4. Relationship between repiquetes, rainfall anomalies and atmospheric circulation

Using a composite analysis, rainfall anomalies from CHIRPS and TRMM datasets were generated for each repiquete type. The same procedure was applied considering low-level (850 hPa) horizontal winds from ERA-Interim reanalysis data. For each repiquete type, daily rainfall anomalies and horizontal wind anomalies at 850 hPa were calculated from 10 days before (d-10) to the first day after (d+1) the repiquete event, taking as day zero (d0) the beginning day of the event at the Tamshiyacu station.

The anomalies were computed considering monthly climatology (the 1997–2017 period for CHIRPS, 1998–2017 for TRMM and 1997–2017 for ERA-Interim datasets). Only significant anomalies higher than a standard deviation within the study period were analyzed for the annual recession. On the other hand, we used the large-scale atmospheric circulation patterns (CPs) defined by Paccini et al. (2017) to identify the main meteorological features involved in these events from d-10 to d+1.

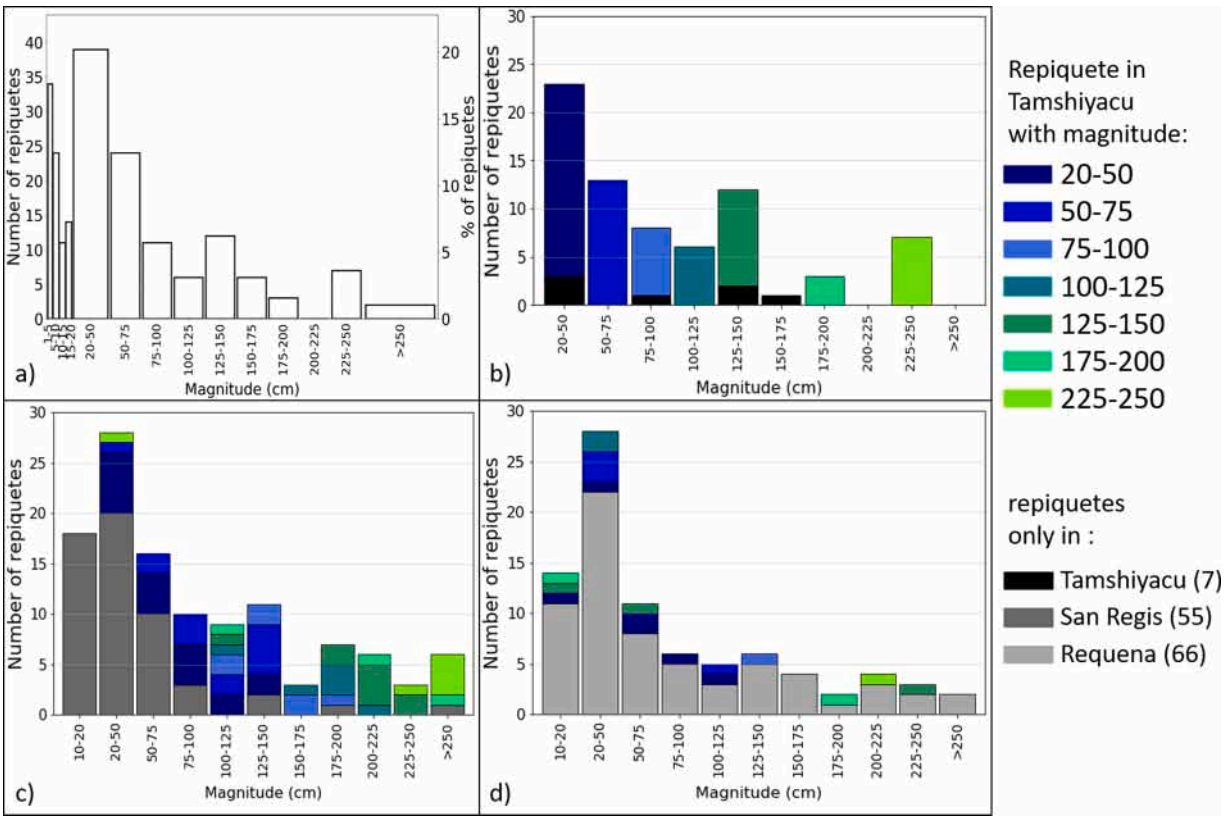

Fig. 2. a) Number of repiquetes as a function of the magnitude of the reversal of river stage at Tamshiyacu station for the 1985–2018 period. b) Number of repiquetes greater than 20 cm at Tamshiyacu station for the common 1996–2018 period. c) Number of repiquetes greater than 10 cm at San Regis station for the common 1996–2018 period. d) Number of repiquetes greater than 10 cm at Requena station for the common 1996–2018 period. Blue to green colors links the magnitude of repiquetes in Tamshiyacu with magnitudes in upstream repiquetes (San Regis or Requena). (For interpretation of the references to colour in this figure legend, the reader is referred to the web version of this article.)

3. Results

3.1. Main hydrological features of repiquetes

For the period 1985–2018, Tamshiyacu gauging station recorded 193 repiquetes (Fig. 2a). The distribution of repiquetes according to their magnitude shows a total of 83 repiquetes lower than 20 cm (i.e. 43 % of the total repiquetes). In addition, the remaining 57 % are grouped into larger intervals: 110 events are greater than 20 cm, 71 greater than 50 cm, 36 greater than 1 m and nine greater than 2 m.

Within the common period analyzed for the three rivers, and considering as significant only those repiquetes that exceed the thresholds of 20 cm in Tamshiyacu and 10 cm in San Regis and Requena stations, only 73, 117 and 85 repiquetes are found in Tamshiyacu, San Regis and Requena stations, respectively (Figs. 2b–d and circles in Fig. 3a). Among these 73 events for Tamshiyacu, only seven repiquetes (10 %) occur without any previous upstream event (Type 4 repiquetes; shown in black in Figs. 2b and 3b). Meanwhile, 66 repiquetes (90 %) greater than 20 cm were previously observed upstream, of which 64 % are Type 1 repiquetes (with a precursor in the Marañón River), 5 % Type 2 repiquetes (with a precursor in the Ucayali River) and 21 % Type 3 repiquetes (with precursors in both tributaries). The other colors in Fig. 2b characterize repiquete events in Tamshiyacu greater than 20 cm and are chosen to compare the differences in magnitude between these events and relate them to the magnitude of events observed upstream (in San Regis or Requena station, Figs. 2c and d). That means that a given color links upstream events with downstream events. 15

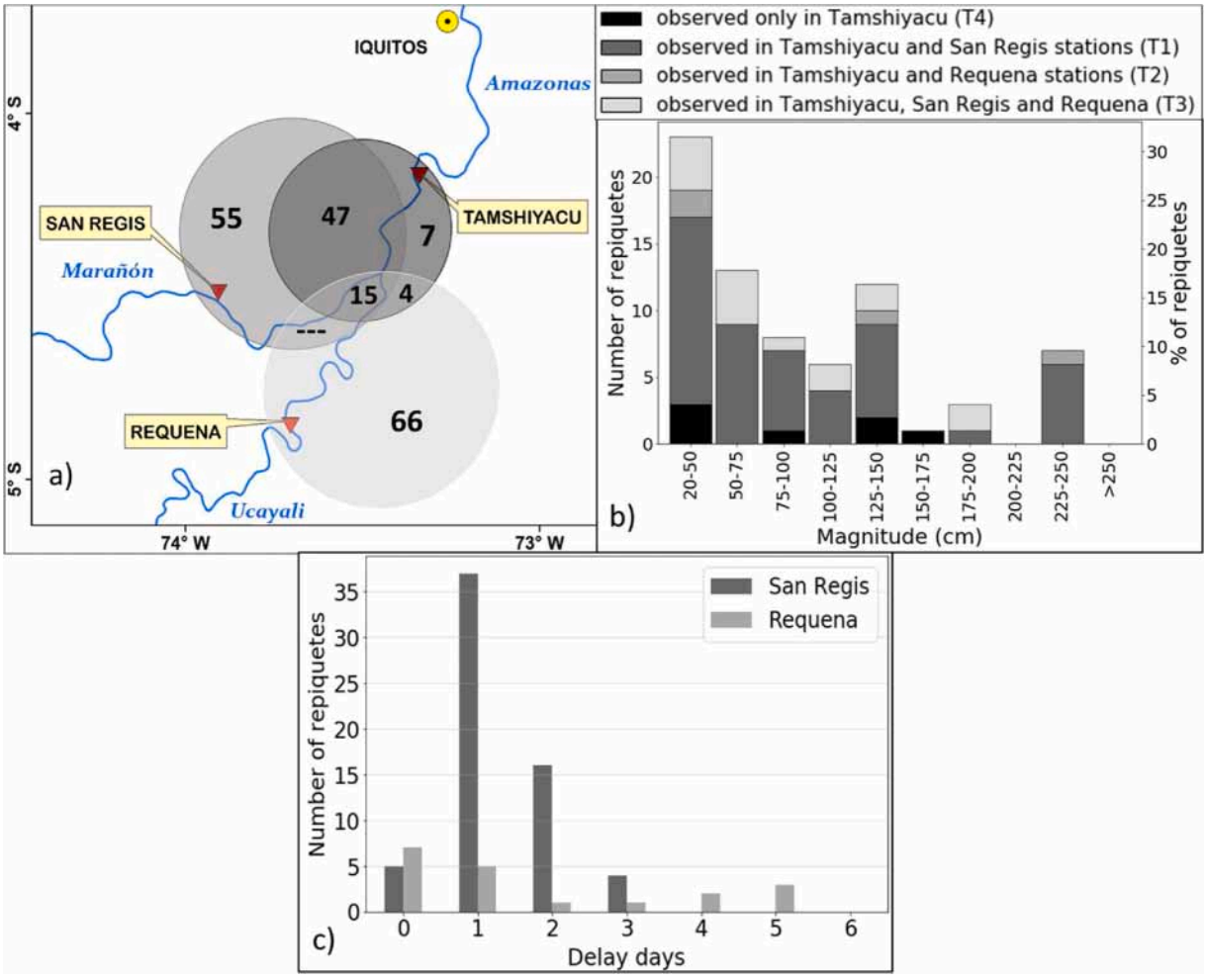

Fig. 3. a) Schematic representation of the number of repiquetes at each gauging station for the 1996–2018 period. The dark gray circle, gray circle and light gray circle correspond to Tamshiyacu, San Regis and Requena, respectively. The intersection of the three circles corresponds to Type 3 repiquetes identified in this study, i.e., the 15 repiquetes observed in Amazonas River with a precursor in the Marañón or the Ucayali Rivers. b) Number of repiquetes with a magnitude greater than 20 cm (73/134 repiquetes) at Tamshiyacu station for the 1996-2018 common period. Magnitude of types of repiquetes in Tamshiyacu station in gray tones. c) Number of repiquetes observed at Tamshiyacu station (Y-axes) and the corresponding delay (X-axes, in days) from the start of repiquetes observed at San Regis (Type 1 and 3) or Requena (Type 2 and 3) stations for the 1996–2018 period.

Repiquetes detected in both Marañón and Ucayali Rivers impact Tamshiyacu station in preceding days (Type 3 repiquetes, intersection between three circles in Fig. 3a). The main differences in Figs. 2b and c for this period, in contrast with the 1985–1995 period, are a higher occurrence of repiquetes with magnitudes higher than 100 cm (0.5 times more in Amazonas River and more than double in Marañón River) and a higher occurrence of repiquetes only observed in a specific station (Tamshiyacu or San Regis).

In the San Regis gauging station, 62 out of 117 repiquetes impact Tamshiyacu (intersection between the dark gray and gray circles in Fig. 3a), where there are 47 Type 1 repiquetes, which happen first in San Regis and some days later in the Amazonas River at Tamshiyacu. No events between 10 and 20 cm in San Regis are affecting Tamshiyacu (first column in Fig. 2c). Moreover, by analyzing blue and green tones in Figs. 2b and c, it appears that most events greater than 1 m and 1.75 m registered in San Regis will systematically cause events that exceed 20 cm and 1 m in Tamshiyacu, respectively (same colors for the related events in Figs. 2b and c).

Regarding the repiquetes in Requena, 19 out of 85 events greater than 10 cm (see colored events in Fig. 2d, or intersection between dark gray and light gray circles in Fig. 3a) are identified as precursors to the repiquetes in Tamshiyacu, of which four are Type 2 repiquetes. The distribution is very similar to that of the other stations.

Figs. 3a and b summarize information about the precursor of repiquetes in Tamshiyacu station. The 47 Type 1 repiquetes (events observed in Tamshiyacu and San Regis) and the 15 Type 3 repiquetes (events found in Tamshiyacu, San Regis and Requena) are studied in more detail in the following sections.

In summary, the main precursor of observed repiquetes (greater than 20 cm) in Tamshiyacu in the Amazonas River is the Marañón River, and there is typically a day of delay (Fig. 3c) between the events registered in San Regis and Tamshiyacu gauging stations. On the other hand, repiquetes in the Ucayali River do not show a clear delay with respect to events in Tamshiyacu (Fig. 3c).

Table 2 shows that for Type 1 repiquetes, the precursor events in the Marañón River are greater than repiquetes in Amazonas River by almost 60 cm, with a duration of 14 and 12 days, respectively. Similar results are found in the four Type 2 repiquetes. For Type 3 repiquetes, there are notable differences between the Marañón and Ucayali Rivers, with a higher magnitude in the case of the former. The median duration at Tamshiyacu is the longest, reaching 13 vs 9 days in upstream stations. The Type 4 repiquetes (only observed in Tamshiyacu station) have an average close to one meter, but their duration of eight days is the shortest among the four repiquete types.

Figs. 4a and b show the monthly variation of the characteristics for Types 1, 2 and 3 repiquetes. Types 1 and 2 are associated with higher magnitudes in September and October with the first quartile above 50 cm. Types 1 and 3 display high duration values in June including outliers. But values higher than 60 days only begin in July, resulting from a combination of both tributaries (T3).

Finally, repiquetes in Tamshiyacu higher than 20 cm are more frequent from the second fortnight of June until the second fortnight of September (Fig. 4c). At the Tamshiyacu station, there is an average of 3.2 repiquetes per year higher than 20 cm. The occurrence of repiquetes higher than 10 cm in the Marañón River is prevalent when compared to the Ucayali River during the critical phases of crops (from June 15th to September 31st), with an average of 5.1 vs 3.7 repiquetes per year. However, in the Ucayali River, the occurrence of repiquetes is variable with less events from July to September. Regarding the Amazonas River, the repiquetes are more frequent between August and September.

3.2. *Rainfall and atmospheric circulation anomalies related to repiquetes*

The 15 events categorized as Type 3 (events in Tamshiyacu that are observed previously in San Regis and Requena) show northeasterly low-level winds in the Peruvian and Ecuadorian Amazon during d-10 and d-9, with negative rainfall anomalies over the Marañón basin and no significant rainfall anomalies over the Ucayali basin (Fig. 5). From d-8 to d-6, northerly cross-equatorial low-level winds are intensified, and easterly wind anomalies are strengthened over the Colombian and Ecuadorian Amazon region, unlike d-9. These wind anomalies are associated with positive rainfall anomalies over the Ecuadorian Amazon-Andes transition region above 500 masl during d-8. In the following days (d-7 and d-6), the low-level circulation is similar to that of d-8 but there are low rainfall anomalies.

From d-5 to d-3 a change in low-level wind anomalies can be observed, characterized by a strong convergence of northerly wind anomalies with southern wind incursion resulting from anticyclonic anomalous circulation over Argentina near 30 °S and 67 °W at

Table 2
Median duration (days) and median magnitude (cm) of the significant repiquetes observed in Amazonas, Marañóón and Ucayali Rivers; and N is the number of repiquetes by station.

		Tamshiyacu Amazonas	San Regis Marañón	Requena Ucayali
T1	N	47	47	–
	Magnitude	81	139	–
	Duration	14	12	–
T2	N	4	–	4
	Magnitude	82	–	138.5
	Duration	13	–	11
T3	N	15	15	15
	Magnitude	74	111	49
	Duration	13	9	9
T4	N	7	–	–
	Magnitude	87	–	–
	Duration	8	–	–

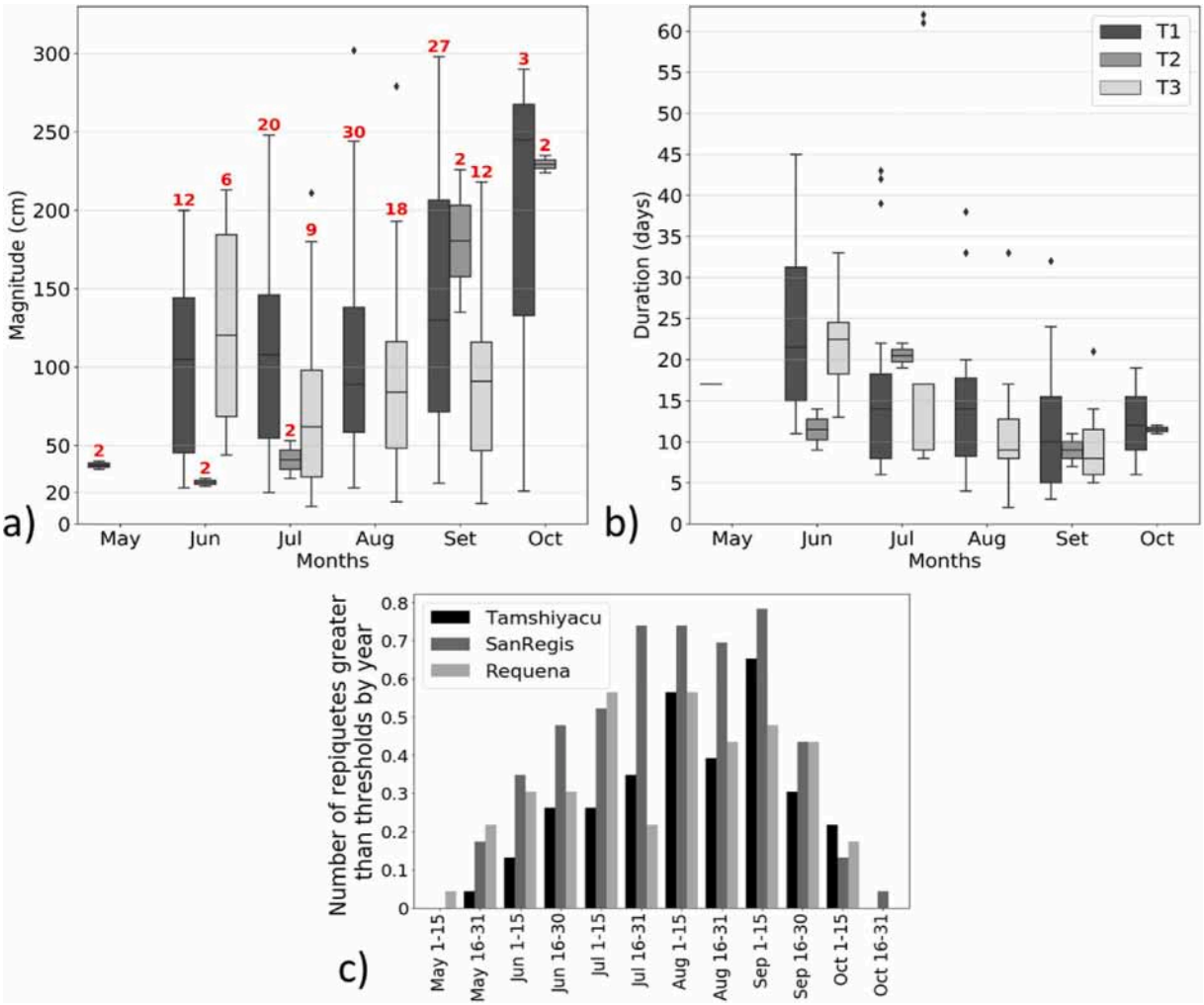

Fig. 4. Monthly variation of a) magnitude (cm) and b) duration (days) of types of repiquetes related to Tamshiyacu station (1996–2018). In red, the number of repiquetes of summarized data in the boxplot, the same numbers are valid to the right boxplot. c) Average (1996–2018) annual number of repiquetes higher than thresholds (20 cm in Tamshiyacu, 10 cm in San Regis and Requena), by fortnight. Gray tones in c correspond to events in each river in contrast to a and b, which correspond to the types of repiquetes.

low-level (Fig. 6). These atmospheric features are characteristic of southerly wind incursions to the East of the Andes, which promote positive rainfall anomalies from the Bolivian Amazon and produce cold surges penetration into the Amazon basin (Garreaud and Wallace, 1998; Espinoza et al., 2012, 2013; Paccini et al., 2017). During these days, high positive rainfall anomalies are observed in the Andes-Amazon transition region between Peru and Ecuador (Figs. 5 and 6). Abundant rainfall is probably due to interactions between local convective processes over the equatorial Andean topography and to large-scale wind convergence between southeasterly and northeasterly wind anomalies over this region (particularly clear in d-5 and d-4, Fig. 6). According to these features, during d-3 a predominance of easterly and southeasterly wind anomalies over the northern equatorial Amazon is associated with positive rainfall anomalies over the northern Marañón basin in the northern Amazon basin (Fig. 6). In addition, enhanced southerly wind anomalies over the Bolivian Amazon are associated with positive rainfall anomalies moving northward to the central and southern Peruvian Amazon in the central Ucayali basin. On d-3, southerly wind anomalies reach the northern Peruvian Amazon while positive rainfall anomalies decrease over the lower Ucayali basin and most of the Marañón basin.

During d-2 and d-1 there are southeasterly wind anomalies over the Peruvian and western Brazilian Amazon, and low positive rainfall anomalies over the central Ucayali (d-2) and Marañón (d-1) basins. Finally, d0 and d+1 are characterized by a weakening of the southerly wind anomalies, while westerly wind anomalies prevail over the northern region, this feature being opposite to the pattern observed during rainy days. These atmospheric patterns reduce the convective activity over the Peruvian and Ecuadorian Amazon, which reduces rainfall over the northern Marañón basin and dries up the Ucayali basin.

Similar rainfall patterns are observed by performing the same analysis with the TRMM dataset (Fig. S2). For instance, the days with more intense positive rainfall anomalies over the two basins are d-5, d-4 and d-3. However, using the TRMM dataset the positive rainfall anomalies in the northern region (between Peru and Ecuador) are slightly lower, probably due to the lower spatial resolution of

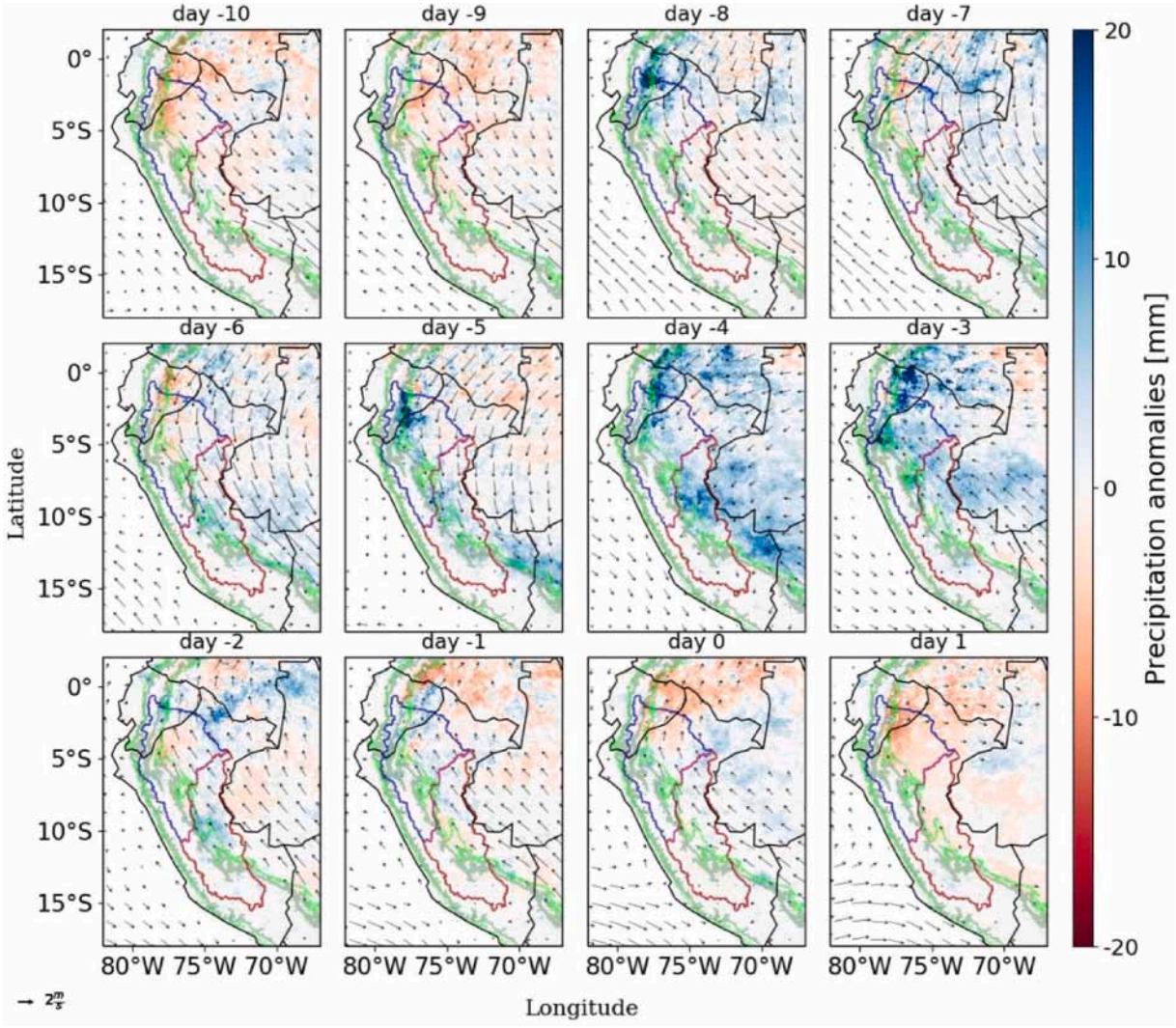

Fig. 5. Composite of 850 hPa winds (ERA-Interim 0.25°) and rainfall (CHIRPS 0.05°) daily anomalies from the preceding ten days (d-10) to the first day (d+1) after the 15 repiquetes observed at Tamshiyacu, San Regis and Requena gauging stations (Type 3) for the 1996–2018 period, taking as day zero (d0) the beginning of the repiquete at Tamshiyacu station. Rainfall and winds anomalies are computed considering monthly mean climatology values averaged for the 1997–2017 period. Green and dark green lines represent elevations of 500 masl and 1500 masl, respectively. Ucayali and Marañón basins are indicated in red and blue, respectively. Only anomalies higher than a standard deviation are showed. (For interpretation of the references to colour in this figure legend, the reader is referred to the web version of this article.)

TRMM.

The 47 events categorized as Type 1 (events in Tamshiyacu that are observed previously only in San Regis) show similar atmospheric patterns to those for events categorized as Type 3, with some relevant differences, described below (Figs. 7 and 8). Days d-10 to d-7 are characterized by weak northwesterly wind anomalies over the Peruvian Amazon and westerly wind anomalies near the equator. These anomalies are related to dry conditions in d-10, d-9, d-8 and d-7 (Fig. 7). During d-6 and d-5, over the northern Marañón basin, there is a change in wind direction from north to the northeast that is associated with the high positive rainfall anomalies in d-5 over the Ecuadorian Andes-Amazon transition region. The following days, d-4 and d-3, are characterized by southeasterly wind anomalies over the Peruvian Amazon plain, but weaker rainfall anomalies (in contrast to Type 3 repiquetes, for which the change from northeasterly to southeasterly winds occurs earlier). In addition, easterly wind anomalies are also observed over the northern region associated with positive rainfall anomalies over the northwestern Amazon basin (Figs. 7 and 8). Finally, from d-2 to d+1, wind anomalies over most of the Tamshiyacu basin are not significant, resulting in no significant rainfall anomaly (Fig. 7).

Similar rainfall patterns to those described in Fig. 7 are observed by performing the same analysis with the TRMM dataset (Fig. S3). But, similar to Type 1 repiquetes analysis, rainfall anomalies are lower in the TRMM dataset in comparison to CHIRPS. As expected, the main difference regarding Type 3 repiquetes is that rainfall is mostly observed in the north (Marañón basin). There is no northeasterly wind anomaly and no convergence with the southeastern advection over the Ucayali, only weak rainfall anomalies carried by the

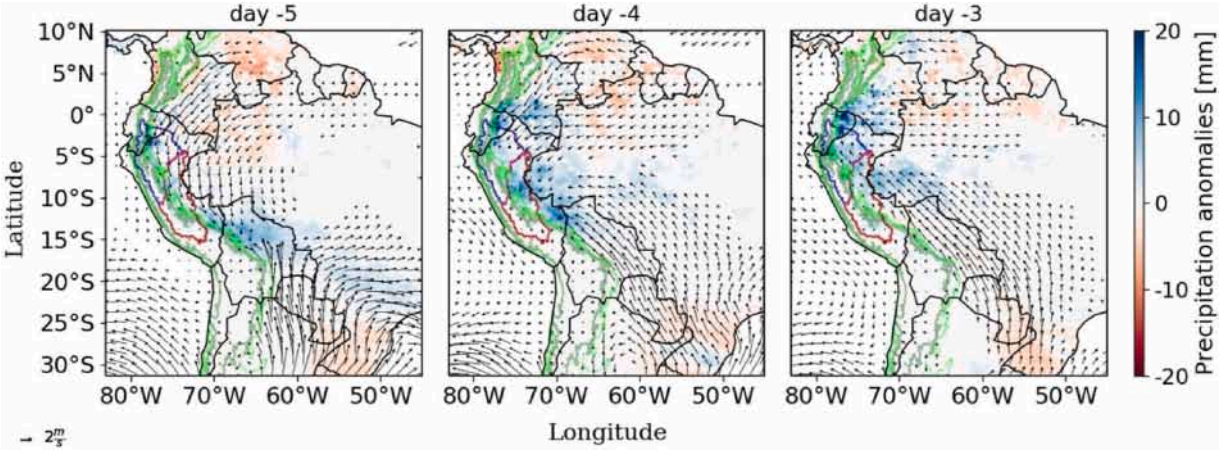

Fig. 6. Same as Fig. 5 but showing rainfall anomalies from the CHIRPS (0.25° × 0.25°) dataset, considering tropical South America during the rainiest days, i.e. from d-5 to d-3.

incursion over this middle basin. As consequence, no repiquetes are reported in the Ucayali River. These atmospheric patterns are coherent with the role of the Marañón River (instead of the Ucayali River) as the precursor of the repiquetes observed in Tamshiyacu.

Furthermore, a longitudinal cross-section of Type 1 repiquetes from 1000 hPa to 200 hPa at 3.25 °S (northern Marañón basin) is shown in Fig. 9. Values of specific humidity greater than 16 g/kg under 925 hPa can be seen from d-8 to d-4. d-6 up to d-4 are characterized by large equivalent potential temperature (EPT) values between 78 °W-73 °W with a smooth decrease in height from the surface to medium levels. This condition is associated with an increase in the velocity of vertical winds from d-5 to d-3 in the eastern Andes. These features suggest atmospheric instability related to enhanced specific humidity, low-level wind convergence forced by the Andes and wind ascendance over the northern Marañón basin during d-5 to d-3, consistent with precipitation patterns observed over this region in Fig. 7.

Table 3 and Table S1 (Supplementary Material) relate each repiquete type to large-scale atmospheric circulation patterns (CPs), previously defined by Paccini et al. (2017), which synthesize the nine main modes of winds variability on an intra-seasonal timescale. In this way, the percentages of days of these CP's occurrence was calculated for each day for each repiquete type. First, for Type 3 repiquetes within the 1997–2014 period (11 out of 15 events), in d-10 and d-9 CP8 is prevailing (36.36 % of the days, apart from other CPs characterized by the northerly wind regime; see Table 3). In the following days, there is a predominance of CP2 (between 45.45 % and 63.64 %) that changes to CP4 in d-2 (36.36 %, apart from other CPs with southerly wind regimes like CP5 and CP6). Therefore, a change from a northerly to a southerly wind regime is evident, especially from 5 to 3 days before to the beginning of the repiquete in Tamshiyacu. However, the easterly flow over the northwest is weak during these CPs, and that could explain why the percentages of days of the occurrence are distributed among other CPs.

4. Discussion

For the first time, our results show the respective influences of the Marañón and Ucayali Rivers on repiquetes in the Amazonas River in terms of magnitude (Figs. 2b–d) and the annual number of repiquetes higher than 10 cm in the Marañón and Ucayali Rivers (Fig. 4c). In addition, the influences of upstream rivers on repiquetes in the Amazonas River in terms of frequency, magnitude, timing and duration are also documented in Figs. 3 and 4. Most of our results regarding frequency, magnitude and duration of repiquetes in the Peruvian Amazonas River are in accordance with previous studies including the average of 3.2 repiquetes per year higher than 20 cm (Coomes et al., 2016; Ronchail et al., 2018). However, in this study, we use a different definition of the recession period based on the annual maximum and minimum water levels (see Section 2) and consider a longer period (4 more years than the studies mentioned).

Regarding the delay between the repiquetes in Tamshiyacu and those in its tributaries, a greater lag can be seen in Requena (Ucayali River as precursor) than San Regis (Marañón River as precursor), up to six days compared to four days. These results and the major influence of the Marañón River on the repiquetes in the Amazonas River during June-October are related to the higher discharge of the Marañón River (almost twice the discharge of the Ucayali River) due to the presence of rainfall in the northern Amazon from June to September. They also are related to the vast floodplains that characterize the Ucayali River and the numerous oxbow lakes around its main channel, to which excess water flows before reaching the Amazonas River (Abizaid, 2005; Coomes et al., 2009; Abad et al., 2013; Armijos et al., 2013). Despite the rapid transfer of water from tributaries to the main stream, this lag between stations could be used to warn downstream farmers not to use valuable seeds (and not waste their time and money). However, to develop a reliable hydrological information service for farmers, the magnitude and duration of repiquetes in the seeding period (June-July) would need to be considered and also their possible negative impacts on the early growing season. On the other hand, higher magnitudes observed in type 2 repiquetes in September and October are related to increased discharges from the Ucayali River at the beginning of the hydrological year caused by the onset of the SAMS from mid-August to early December (Arias et al., 2015).

Changes from northerly to southerly anomalies in low-level winds are related to precipitation 3–5 days before the occurrence of

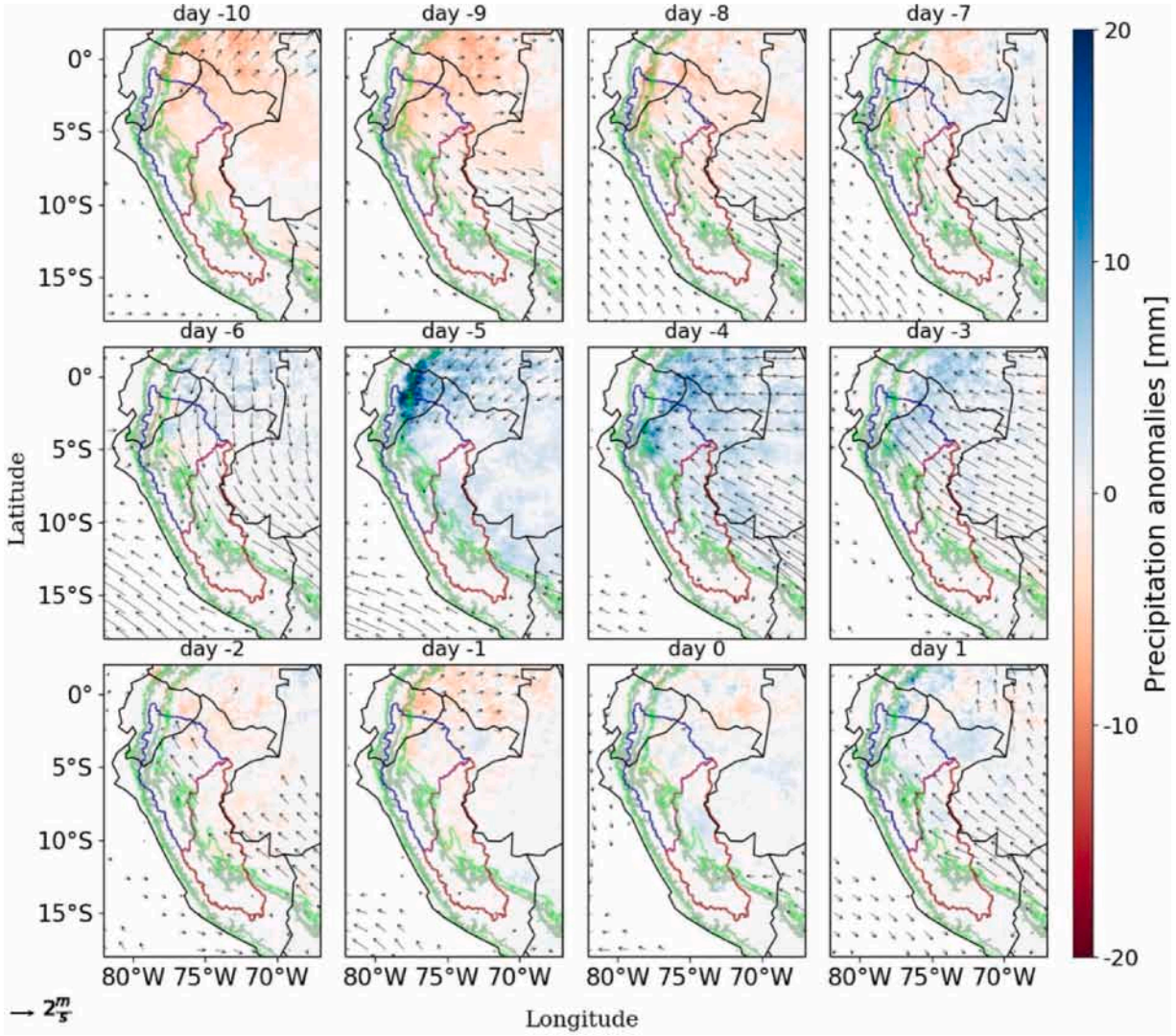

Fig. 7. Composite of 850 hPa winds (ERA-Interim 0.25°) and rainfall (CHIRPS 0.05°) daily anomalies from the preceding ten days (d-10) to the first day after (d+1) of the 47 observed repiquete events at Tamshiyacu and San Regis stations (Type 1) for the 1996–2018 period, taking as day zero (d0) the beginning day of the repiquetes at Tamshiyacu station. Rainfall and winds anomalies are computed considering monthly mean climatology values averaged for the 1997–2017 period. Green lines and dark green lines represent elevations of 500 masl and 1500 masl, respectively. Ucayali and Marañón basins are indicated in red and blue, respectively. Only anomalies higher than a standard deviation are showed. (For interpretation of the references to colour in this figure legend, the reader is referred to the web version of this article.)

repiquetes. Previous studies have documented that southeastern flux and intense precipitation over the north-western Amazon are related to anomalous anticyclonic circulations in eastern Bolivia, the eastward displacement of extra-tropical systems and equatorial circulations (Wang and Fu, 2002; Santos et al., 2015; Paccini et al., 2017). Besides, in some cases, these fluxes could be related to cold surges with high surface pressures (Espinoza et al., 2013). However, our study provides new information regarding the main atmospheric processes associated with repiquetes in the Peruvian Ecuadorian Amazon. In particular, positive rainfall anomalies over the northern Marañón basin are a common feature observed days before the start of the repiquete. Enhanced convective activity over the northern Marañón basin is related to southerly wind incursions and an intensification of easterly low-level winds, which transport moisture from the central Amazon to the western Amazon basin. Thus, low-level wind convergence forced by the Andean topography are observed over the northern Marañón basin from five to three days before the start of the repiquete in Tamshiyacu (Fig. 9).

Previous studies found a strong relationship between wind circulation and rainfall patterns on a monthly and intraseasonal scale in the upper Amazon basin (e.g. Paccini et al., 2017; Mayta et al., 2018). However, wind circulation is better represented in atmospheric models than precipitation, particularly over the Andes (Minvielle and Garreaud, 2011); therefore, the use of wind circulation would be useful to predict repiquetes events. Furthermore, our results are fundamental to the development of measures to help farmers cope with flood reversals. The forecast of repiquetes generally occurs too late, so they inevitably flood newly-seeded fields, choke the young

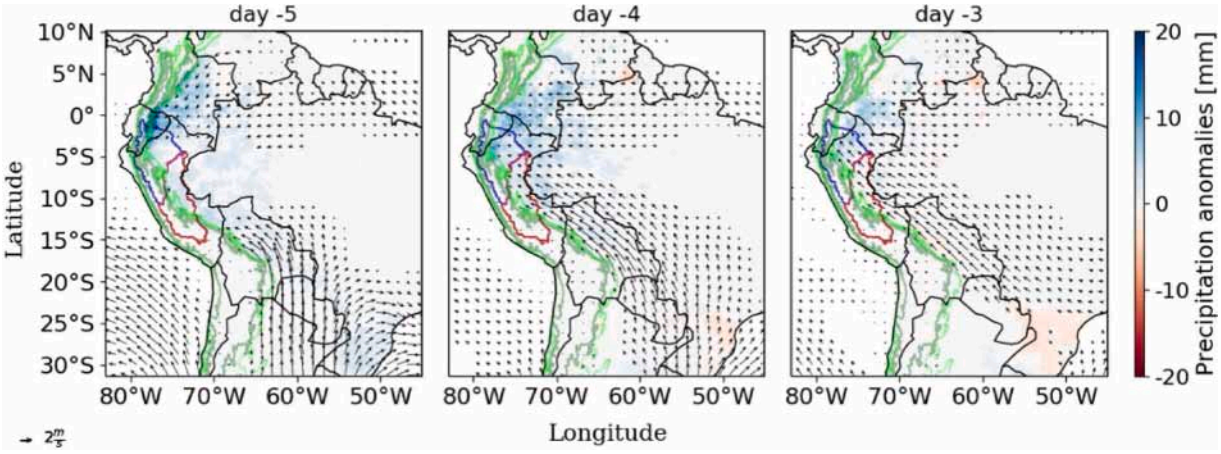

Fig. 8. Same as Fig. 7 but showing rainfall anomalies from the CHIRPS (0.25°x 0.25°) dataset, considering tropical South America during the rainiest days, i.e. from d-5 to d-3.

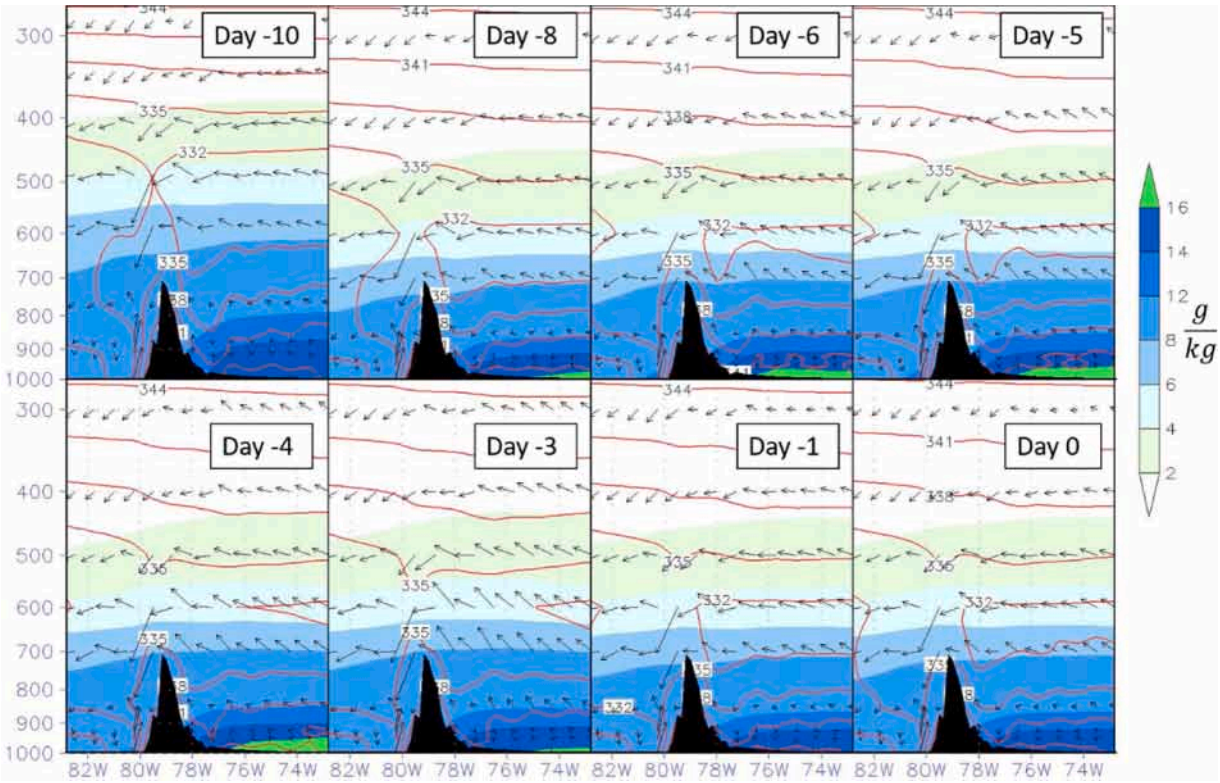

Fig. 9. Pressure-Longitude cross-section (3.25 °S) of specific humidity (g/kg, in colors shaded), equivalent potential temperature (K, in red lines each 3 K) and zonal-vertical wind (cm/s) composites of repiquetes type T1 from d-10 to d0. The Andes are represented in black.

plants with sediment, and shorten the growing season, which is a significant impediment to the development of the agricultural potential of the lowlands in western Amazonia. However, the beginning of the seeding period (June–July) is crucial when prediction could be useful for avoiding unproductive seeding. So, it will be necessary to improve atmospheric and hydrological forecasts focusing on prevention during the beginning of the crop period before farmers plant theirs seeds, forecasting repiquetes in June and July. For this purpose, we encourage future research with this approach, combined with the implementation of regional scales 1D/2D hydrological models (Wongchuig Correa et al., 2017). Another alternative to improve the accuracy of short-term streamflow forecasting hybrid models which have recently been developed (Pramanik et al., 2011; Santos et al., 2014; Vergara and Lavado, 2016) is the use of data about atmospheric patterns as input to improve these models, as they are less uncertain than precipitation.

Table 3
Percentages of days (%) of the occurrence of large-scale circulation patterns (CPs, defined by Paccini et al., 2017) from d-10 to d0 during Type 3 repiquetes (observed in Tamshiyacu with precursors in both tributaries) of 11/15 observed events for the 1997 – 2014 period. Values greater than 20 % are in bold, and all values greater than 35 % are underlined.

CP	−10d	−9d	−8d	−7d	−6d	−5d	−4d	−3d	−2d	−1d	0d
1	18.18	0.00	0.00	0.00	0.00	0.00	0.00	0.00	0.00	0.00	0.00
2	9.09	18.18	**45.45**	**45.45**	**63.64**	**27.27**	0.00	18.18	0.00	0.00	0.00
3	18.18	0.00	9.09	18.18	9.09	9.09	**27.27**	9.09	9.09	18.18	9.09
4	0.00	0.00	0.00	9.09	9.09	9.09	18.18	**27.27**	**36.36**	**27.27**	18.18
5	0.00	18.18	9.09	0.00	0.00	0.00	0.00	9.09	9.09	**36.36**	**36.36**
6	9.09	**27.27**	18.18	0.00	9.09	9.09	**27.27**	18.18	**27.27**	18.18	**27.27**
7	9.09	0.00	0.00	9.09	9.09	9.09	0.00	0.00	0.00	0.00	0.00
8	**36.36**	**36.36**	18.18	18.18	0.00	18.18	9.09	9.09	18.18	0.00	9.09
9	0.00	0.00	0.00	0.00	0.00	18.18	18.18	9.09	0.00	0.00	0.00

A limitation in this study is the lack of additional time series of water level data which could be solved by combining remote sensing techniques and the use of virtual stations based on altimetry satellites and synthetic aperture radar (SAR) applications which can measure the extent of floods and changes in water level (e.g. Wdowinski et al., 2008; Ovando et al., 2016; Häfliger et al., 2019). Nevertheless, it is necessary to consider that this work does not analyze factors like fluvial morpho-dynamics and groundwater anomalies that could affect repiquete events.

Moreover, some projections based on the western Amazon indicated a future increase in the frequency of wet years and increased mean and maximum discharges along the Peruvian floodplain (Guimberteau et al., 2013; Langerwisch et al., 2013; Sorribas et al., 2016; Zulkafli et al., 2016). These changes could affect the frequency, seasonality, duration and magnitude of repiquetes as well.

5. Conclusions

This work investigates the frequency, magnitude and timing of river stage recessional reversals known as “repiquetes” along the Peruvian Amazon River and its two formative tributaries, the Ucayali and Marañón Rivers. Water-level data is used to understand the influence of upstream tributaries as precursors of repiquetes in the Amazonas River and to classify the occurrence of reversals higher than 20 cm in the Amazonas and higher than 10 cm in the tributaries into types according to their origin. As a result, Type 1 repiquetes (repiquetes in the Amazonas River with a precursor in the Marañón River) are the most frequent (64 % of the total significant repiquetes in the Amazonas River) while repiquetes in the Amazonas River with a precursor in the Ucayali River (Type 2) are much less frequent (5 %). Thus, the study shows that repiquetes in the Marañón River are the primary precursors of repiquetes in the Amazonas River; this is consistent with the fact that rains can occur during the winter months in the Marañón basin, which is much rarer in the Ucayali basin. Moreover, precursors in the Marañón River greater than 1 m will systematically cause repiquetes higher than 20 cm in the Amazonas River. On average, repiquetes in the Marañón River occur one day before those observed in the Amazonas River and most last around 12 days. However, the Ucayali River has an increasing influence on the frequency and magnitude of repiquetes in September and October due to the beginning of the hydrological year in the southern tropical Amazon basin.

This study identifies rainfall and large-scale atmospheric circulation patterns related to the occurrence of repiquetes events. It focuses on hydro-meteorological conditions related to Type 1 and Type 3 repiquetes (repiquetes in the Amazonas River with a precursor in both tributaries), and rainfall anomalies which were analyzed from ten days before (d-10) to the beginning day of repiquetes (d0) in Tamshiyacu station (Amazonas River). We found that the Peruvian and Ecuadorian Andes-Amazon transition region in the northern Marañón basin is a key region that presents positive rainfall anomalies from five to three days before the repiquete (d-5 to d-3). The positive rainfall anomalies are associated with changes in low-level circulations patterns in the days leading up to the repiquete. In general, there is a progressive intensification of the northerly flow from d-10 to d-7 over the equatorial region, followed by a clear low-level northerly to southerly winds change between d-5 and d-3 supported by an easterly flow. During these days, convergence forced by the presence of the Andes is observed in the northern Marañón basin, which enhanced convective activity over this region. Repiquetes with precursors in both rivers (Type 3) are characterized by a strong convergence between intense northeasterly winds and southerly winds over the northern and central Tamshiyacu basin from d-5 to d-3. However, in Type 1 repiquetes, northeasterly winds are weaker than in Type 3 and wind convergence is predominant only in the northern Marañón basin.

This study shows the origin of repiquetes upstream of Tamshiyacu station and their connection with atmospheric patterns. These results encourage further analysis regarding other factors like fluvial morpho-dynamics and groundwater anomalies that could affect repiquete events in order to improve the forecast of such events, which principally have an atmospheric origin. While the lack of gauge data remains a major limitation, new information (mainly based on remotely sensed observations) will supply water surface elevations covering more river sections with better spatial and temporal resolution. In addition to this, the major application of our results is to give alternatives to improve the accuracy of short-term streamflow forecasting during the annual recession using atmospheric patterns that could be inputted to hybrid models for recently developed short-term streamflow forecasting.

These results are fundamental to the development of measures to help farmers deal with repiquetes, and they can be added to the efforts to obtain a secure flood index or hydrological services for farmers focusing on the periods before and during planting considering the fragility of seeds and young plants.

CRediT authorship contribution statement

Manuel Figueroa: Conceptualization, Methodology, Software, Validation, Formal analysis, Investigation, Resources, Data curation, Writing - original draft, Writing - review & editing, Visualization. **Elisa Armijos:** Conceptualization, Methodology, Software, Formal analysis, Investigation, Resources, Writing - original draft, Writing - review & editing. **Jhan Carlo Espinoza:** Conceptualization, Methodology, Validation, Formal analysis, Investigation, Resources, Writing - original draft, Writing - review & editing. **Josyane Ronchail:** Methodology, Formal analysis, Resources, Writing - original draft, Writing - review & editing. **Pascal Fraizy:** Methodology, Software, Resources, Writing - review & editing.

Declaration of Competing Interest

The authors report no declarations of interest.

Acknowledgements

This research was funded by the N° 412-2019-FONDECYT/BM Project and JCE received the support of the French AMANECER-MOPGA project funded by ANR and IRD (ref. ANR-18-MPGA-0008). Special thanks to the N° 010-2018-FONDECYT/BM MoSARD Project. We also thank the HYBAM observatory for providing the hydrological series. The data used in this paper were acquired from Goddard Earth System division and Information Service Center [TRMM 3B42; https://disc.sci.gsfc.nasa.gov/], Climate Hazards Group [CHIRPS; https://chc.ucsb.edu/data/chirps/] and ECMWF [ERA Interim reanalysis; https://apps.ecmwf.int/datasets/]. We would also like to show our gratitude to our colleagues Victor Chávez, Gerardo Rivera and Raúl Espinoza, who provided insight and expertise that greatly assisted the research. Finally, we are very grateful to Nicole Chabaneix because her brilliant work and comments have improved the quality of publishing of our study.

Appendix A. Supplementary data

Supplementary material related to this article can be found, in the online version, at doi:https://doi.org/10.1016/j.ejrh.2020.100752.

References

Abad, J.D., Vizcarra, J., Paredes, J., Montoro, H., Frias, C., Holguin, C., 2013. Morphodynamics of the upper Peruvian Amazonian rivers, implications into fluvial transportation. Int. Conf. IDS2013 - Amaz. 1–10.

Abizaid, C., 2005. An anthropogenic meander cutoff along the Ucayali River, Peruvian Amazon. Geogr. Rev. 95, 122–135. https://doi.org/10.1111/j.1931-0846.2005.tb00194.x.

Ampuero, A., Vuille, M., Novello, V.F., Cruz, F.W., Vonhof, H., Mayta, V.C., Campello, R.C., Siffedine, A., Fluminense, U.F., 2020. The forest effects on the isotopic composition of rainfall in the northwestern Amazon Basin. J. Geophys. Res. Atmos. 125 https://doi.org/10.1029/2019JD031445.

Arias, P.A., Fu, R., Vera, C., Rojas, M., 2015. A correlated shortening of the North and South American monsoon seasons in the past few decades. Clim. Dyn. 45, 3183–3203. https://doi.org/10.1007/s00382-015-2533-1.

Armijos, E., Crave, A., Vauchel, P., Fraizy, P., Santini, W., Moquet, J.S., Arevalo, N., Carranza, J., Guyot, J.L., 2013. Suspended sediment dynamics in the Amazon River of Peru. J. South Am. Earth Sci. 44, 75–84. https://doi.org/10.1016/j.jsames.2012.09.002.

Chavez, S.P., Takahashi, K., 2017. Orographic rainfall hot spots in the Andes-Amazon transition according to the TRMM precipitation radar and in situ data. J. Geophys. Res. 122, 5870–5882. https://doi.org/10.1002/2016JD026282.

Coomes, O.T., Abizaid, C., Lapointe, M., 2009. Human modification of a large meandering Amazonian River: genesis, ecological and economic Consequences of the Masisea Cutoff on the Central Ucayali. Peru. Ambio 38, 130–134. https://doi.org/10.1579/0044-7447-38.3.130.

Coomes, O.T., Lapointe, M., Templeton, M., List, G., 2016. Amazon river flow regime and flood recessional agriculture: flood stage reversals and risk of annual crop loss. J. Hydrol. 539, 214–222. https://doi.org/10.1016/j.jhydrol.2016.05.027.

Dee, D.P., Uppala, S.M., Simmons, A.J., Berrisford, P., Poli, P., Kobayashi, S., Andrae, U., Balmaseda, M.A., Balsamo, G., Bauer, P., Bechtold, P., Beljaars, A.C.M., van de Berg, L., Bidlot, J., Bormann, N., Delsol, C., Dragani, R., Fuentes, M., Geer, A.J., Haimberger, L., Healy, S.B., Hersbach, H., Hólm, E.V., Isaksen, L., Kållberg, P., Köhler, M., Matricardi, M., Mcnally, A.P., Monge-Sanz, B.M., Morcrette, J.J., Park, B.K., Peubey, C., de Rosnay, P., Tavolato, C., Thépaut, J.N., Vitart, F., 2011. The ERA-Interim reanalysis: configuration and performance of the data assimilation system. Q. J. R. Meteorol. Soc. 137, 553–597. https://doi.org/10.1002/qj.828.

Espinoza, J.C., Guyot, J.L., Ronchail, J., Cochonneau, G., Filizola, N., Fraizy, P., Labat, D., de Oliveira, E., Ordoñez, J.J., Vauchel, P., 2009a. Contrasting regional discharge evolutions in the Amazon basin (1974-2004). J. Hydrol. 375, 297–311. https://doi.org/10.1016/j.jhydrol.2009.03.004.

Espinoza, J.C., Ronchail, J., Guyot, J.L., Cochonneau, G., Naziano, F., Lavado, W., de Oliveira, E., Pombosa, R., Vauchel, P., 2009b. Spatio-temporal rainfall variability in the Amazon basin countries (Brazil, Peru, Bolivia, Colombia, and Ecuador). Int. J. Climatol. 29, 1574–1594. https://doi.org/10.1002/joc.1791.

Espinoza, J.C., Ronchail, J., Guyot, J.L., Junquas, C., Vauchel, P., Lavado, W., Drapeau, G., Pombosa, R., 2011. Climate variability and extreme drought in the upper Solimões River (western Amazon Basin): understanding the exceptional 2010 drought. Geophys. Res. Lett. 38, 1–6. https://doi.org/10.1029/2011GL047862.

Espinoza, J.C., Lengaigne, M., Ronchail, J., Janicot, S., 2012. Large-scale circulation patterns and related rainfall in the Amazon Basin: a neuronal networks approach. Clim. Dyn. 38, 121–140. https://doi.org/10.1007/s00382-011-1010-8.

Espinoza, J.C., Ronchail, J., Lengaigne, M., Quispe, N., Silva, Y., Bettolli, M.L., Avalos, G., Llacza, A., 2013. Revisiting wintertime cold air intrusions at the east of the Andes: propagating features from subtropical Argentina to Peruvian Amazon and relationship with large-scale circulation patterns. Clim. Dyn. 41, 1983–2002. https://doi.org/10.1007/s00382-012-1639-y.

Espinoza, J.C., Chavez, S., Ronchail, J., Junquas, C., Takahashi, K., Lavado, W., 2015. Rainfall hotspots over the southern tropical Andes: spatial distribution, rainfall intensity, and relations with large-scale atmospheric circulation. Water Resour. Res. 2498–2514. https://doi.org/10.1002/2015WR017200.A.

Espinoza, J.C., Ronchail, J., Marengo, J.A., Segura, H., 2018. Contrasting North–South changes in Amazon wet-day and dry-day frequency and related atmospheric features (1981–2017). Clim. Dyn. https://doi.org/10.1007/s00382-018-4462-2.

Espinoza, J.C., Garreaud, R., Poveda, G., Arias, P.A., Molina-Carpio, J., Masiokas, M., Viale, M., Scaff, L., 2020. Hydroclimate of the Andes Part I: main climatic features. Front. Earth Sci. 8, 1–20. https://doi.org/10.3389/feart.2020.00064.
Funk, C., Peterson, P., Landsfeld, M., Pedreros, D., Verdin, J., Shukla, S., Husak, G., Rowland, J., Harrison, L., Hoell, A., Michaelsen, J., 2015. The climate hazards infrared precipitation with stations - a new environmental record for monitoring extremes. Sci. Data 2, 1–21. https://doi.org/10.1038/sdata.2015.66.
Garreaud, R.D., Wallace, J.M., 1998. Summertime incursions of midlatitude air into subtropical and tropical South America. Mon. Weather Rev. 126, 2713–2733. https://doi.org/10.1175/1520-0493(1998)126<2713:SIOMAI>2.0.CO;2.
Guevara Díaz, J.M., 2014. Uso correcto de la correlación cruzada en Climatología: el caso de la presión atmosférica entre Taití y Darwin. Terra Nueva Etapa 30, 79–102.
Guimberteau, M., Ronchail, J., Espinoza, J.C., Lengaigne, M., Sultan, B., Polcher, J., Drapeau, G., Guyot, J.L., Ducharne, A., Ciais, P., 2013. Future changes in precipitation and impacts on extreme streamflow over Amazonian sub-basins. Environ. Res. Lett. 8 https://doi.org/10.1088/1748-9326/8/1/014035.
Häfliger, V., Martin, E., Boone, A., Ricci, S., Biancamaria, S., 2019. Assimilation of synthetic SWOT river depths in a regional hydrometeorological model. Water (Switzerland) 11. https://doi.org/10.3390/w11010078.
Hiraoka, M., 1985. Floodplain farming in the Peruvian amazon. Geogr. Rev. Jpn. 58, 1–23. https://doi.org/10.4157/grj1984b.58.1.
Kalliola, R., Salo, J., Puhakka, M., Rajasilta, M., Häme, T., Neller, R.J., Räsänen, M.E., Arias, W.A.D., 1992. Upper amazon channel migration. Naturwissenschaften 79, 75–79. https://doi.org/10.1007/BF01131806.
Kiladis, G.N., Wheeler, M.C., Haertel, P.T., Straub, K.H., Roundy, P.E., 2009. Convectively coupled equatorial waves in reanalysis data. 1–22. https://doi.org/10.1029/2008RG000266.1.HISTORICAL.
Killeen, T.J., Douglas, M., Consiglio, T., Jørgensen, P.M., Mejia, J., 2007. Dry spots and wet spots in the Andean hotspot. J. Biogeogr. 34, 1357–1373. https://doi.org/10.1111/j.1365-2699.2006.01682.x.
Langerwisch, F., Rost, S., Gerten, D., Poulter, B., Rammig, A., Cramer, W., 2013. Potential effects of climate change on inundation patterns in the Amazon Basin. Hydrol. Earth Syst. Sci. 17, 2247–2262. https://doi.org/10.5194/hess-17-2247-2013.
Laraque, A., Ronchail, J., Cochonneau, G., Pombosa, R., Guyot, J.L., 2007. Heterogeneous distribution of rainfall and discharge regimes in the Ecuadorian Amazon basin. J. Hydrometeorol. 8, 1364–1381. https://doi.org/10.1175/2007JHM784.1.
Lavado Casimiro, W.S., Labat, D., Ronchail, J., Espinoza, J.C., Guyot, J.L., 2013. Trends in rainfall and temperature in the Peruvian Amazon-Andes basin over the last 40years (1965–2007). Hydrol. Process. 27, 2944–2957. https://doi.org/10.1002/hyp.9418.
Lee, L.J.E., Lawrence, D.S.L., Price, M., 2006. Analysis of water-level response to rainfall and implications for recharge pathways in the Chalk aquifer, SE England. J. Hydrol. 330, 604–620. https://doi.org/10.1016/j.jhydrol.2006.04.025.
List, G., 2016. Agriculture and the Risk of Crop Loss in the Amazon River Floodplain of Peru. McGill University.
List, G., Coomes, O.T., 2017. Natural hazards and risk in rice cultivation along the upper Amazon River. Nat. Hazards 87, 165–184. https://doi.org/10.1007/s11069-017-2758-x.
Marengo, J.A., Soares, W.R., Saulo, C., Nicolini, M., 2004. Climatology of the low-level jet east of the Andes as derived from the NCEP-NCAR reanalyses: characteristics and temporal variability. J. Clim. 17, 2261–2280. https://doi.org/10.1175/1520-0442(2004)017<2261:COTLJE>2.0.CO;2.
Mayta, V.C., Ambrizzi, T., Espinoza, J.C., Silva Dias, P.L., 2018. The role of the Madden–Julian oscillation on the Amazon Basin intraseasonal rainfall variability. Int. J. Climatol. 39, 343–360. https://doi.org/10.1002/joc.5810.
McClain, M.E., Naiman, R.J., 2008. Andean influences on the biogeochemistry and ecology of the Amazon River. Bioscience 58, 325–338. https://doi.org/10.1641/b580408.
Minvielle, M., Garreaud, R.D., 2011. Projecting rainfall changes over the South American Altiplano. J. Clim. 24 (17), 4577–4583. https://doi.org/10.1175/JCLI-D-11-00051.1.
Ovando, A., Tomasella, J., Rodriguez, D.A., Martinez, J.M., Siqueira-junior, J.L., Pinto, G.L.N., Passy, P., Vauchel, P., 2016. Extreme flood events in the Bolivian Amazon wetlands. J. Hydrol. Reg. Stud. 5, 293–308. https://doi.org/10.1016/j.ejrh.2015.11.004.
Paccini, L., Espinoza, J.C., Ronchail, J., Segura, H., 2017. Intra-seasonal rainfall variability in the Amazon basin related to large-scale circulation patterns: a focus on western Amazon–Andes transition region. Int. J. Climatol. 38, 2386–2399. https://doi.org/10.1002/joc.5341.
Pramanik, N., Panda, R.K., Singh, A., 2011. Daily river flow forecasting using wavelet ANN hybrid models. J. Hydroinform. 13, 49–63. https://doi.org/10.2166/hydro.2010.040.
Recalde-Coronel, G.C., Zaitchik, B., Pan, W.K., 2020. Madden-Julian oscillation influence on sub-seasonal rainfall variability on the west of South America. Clim. Dyn. 1, 3. https://doi.org/10.1007/s00382-019-05107-2.
Rios Arevalo, M., 2005. Agrobiodiversifiacion de playas y barreales y su funcion en la economia familiar ribereña de la Amazonia peruana. Universidade Federal do Pará.
Ronchail, J., Espinoza, J.C., Drapeau, G., Sabot, M., Cochonneau, G., Schor, T., 2018. The flood recession period in Western Amazonia and its variability during the 1985–2015 period. J. Hydrol. Reg. Stud. 15, 16–30. https://doi.org/10.1016/j.ejrh.2017.11.008.
Santos, C.A.G., Freire, P.K.M.M., Silva, G.B.L., Silva, R.M., 2014. Discrete wavelet transform coupled with ANN for daily discharge forecasting into Três Marias reservoir. Proc. Int. Assoc. Hydrol. Sci. 364, 100–105. https://doi.org/10.5194/piahs-364-100-2014.
Santos, E.B., Lucio, P.S., Santos e Silva, C.M., 2015. Synoptic patterns of atmospheric circulation associated with intense precipitation events over the Brazilian Amazon. Theor. Appl. Climatol. 128, 343–358. https://doi.org/10.1007/s00704-015-1712-7.
Satyamurty, P., Nobre, C.A., Silva Dias, P.L., 1998. South America. In: Karoly, D., Vincent, D. (Eds.), Meteorology of the Southern Hemisphere. Meteorological Monographs, American Meteorological Society. American Meteorological Society, Boston, Massachusetts, pp. 119–139. https://doi.org/10.1175/0065-9401-27.49.1.
Segura, H., Junquas, C., Espinoza, J.C., Vuille, M., Jauregui, Y.R., Rabatel, A., Condom, T., Lebel, T., 2019. New insights into the rainfall variability in the tropical Andes on seasonal and interannual time scales. Clim. Dyn. 53, 405–426. https://doi.org/10.1007/s00382-018-4590-8.
Sorribas, M.V., Paiva, R.C.D., Melack, J.M., Bravo, J.M., Jones, C., Carvalho, L., Beighley, E., Forsberg, B., Costa, M.H., 2016. Projections of climate change effects on discharge and inundation in the Amazon basin. Clim. Change 136, 555–570. https://doi.org/10.1007/s10584-016-1640-2.
Vera, C., Higgins, W., Amador, J., Ambrizzi, T., Garreaud, R., Gochis, D., Gutzler, D., Lettenmaier, D., Marengo, J., Mechoso, C.R., Nogues-Paegle, J., Silva Dias, P.L., Zhang, C., 2006. Toward a unified view of the American monsoon systems. J. Clim. 19, 4977–5000. https://doi.org/10.1175/JCLI3896.1.
Vergara, L.E., Lavado, W.S., 2016. Simulación y pronóstico de caudales diarios del río Amazonas (Tamshiyacu) usando modelo híbrido Wavelet Redes Neuronales. Xxvii Congr. Latinoam. Hidráulica Aiih.
Wang, H., Fu, R., 2002. Cross-equatorial flow and seasonal cycle of precipitation over South America. J. Clim. 15, 1591–1608. https://doi.org/10.1175/1520-0442(2002)015<1591:CEFASC>2.0.CO;2.
Wdowinski, S., Kim, S., Amelung, F., Dixon, T.H., Miralles-wilhelm, F., Sonenshein, R., 2008. Space-Based Detection of Wetlands' Surface Water Level Changes from L-Band SAR Interferometry, vol. 112, pp. 681–696. https://doi.org/10.1016/j.rse.2007.06.008.
Wongchuig Correa, S., de Paiva, R.C.D., Espinoza, J.C., Collischonn, W., 2017. Multi-decadal hydrological retrospective: case study of Amazon floods and droughts. J. Hydrol. 549, 667–684. https://doi.org/10.1016/j.jhydrol.2017.04.019.
Zubieta, R., Getirana, A., Espinoza, J.C., Lavado, W., 2015. Impacts of satellite-based precipitation datasets on rainfall-runoff modeling of the Western Amazon basin of Peru and Ecuador. J. Hydrol. 528, 599–612. https://doi.org/10.1016/j.jhydrol.2015.06.064.
Zulkafli, Z., Buytaert, W., Onof, C., Manz, B., Tarnavsky, E., Lavado, W., Guyot, J.L., 2014. A comparative performance analysis of TRMM 3B42 (TMPA) versions 6 and 7 for hydrological applications over Andean-Amazon river basins. J. Hydrometeorol. 15, 581–592. https://doi.org/10.1175/JHM-D-13-094.1.
Zulkafli, Z., Buytaert, W., Manz, B., Rosas, C.V., Willems, P., Lavado-Casimiro, W., Guyot, J.L., Santini, W., 2016. Projected increases in the annual flood pulse of the Western Amazon. Environ. Res. Lett. 11 https://doi.org/10.1088/1748-9326/11/1/014013.